ADVANCED FUNCTIONAL MATERIALS

Postfach 10 11 61
69451 Weinheim
Germany
Courier services:
Boschstraße 12
69469 Weinheim
Germany
Tel.: (+49) 6201 606 531
Fax: (+49) 6201 606 500
E-mail: afm@wiley.com

WILEY-VCH

Dear Author,

Please correct your galley proofs carefully and return them no more than four days after the page proofs have been received.

Please limit corrections to errors already in the text; cost incurred for any further changes or additions will be charged to the author, unless such changes have been agreed upon by the editor.

The editors reserve the right to publish your article without your corrections if the proofs do not arrive in time.

Note that the author is liable for damages arising from incorrect statements, including misprints.

Please note any queries that require your attention. These are indicated with a Q in the PDF and a question at the end of the document.

Reprints may be ordered by filling out the accompanying form.

Return the reprint order form by fax or by e-mail with the corrected proofs, to Wiley-VCH : **afm@wiley.com**

To avoid commonly occurring errors, **please ensure that the following important items are correct** in your proofs (please note that once your article is published online, no further corrections can be made):

- **Names** of all authors present and spelled correctly
- **Titles** of authors correct (Prof. or Dr. only: please note, Prof. Dr. is not used in the journals)
- **Addresses** and **postcodes** correct
- **E-mail address** of corresponding author correct (current email address)
- **Funding bodies** included and grant numbers accurate
- **Title** of article OK
- All **figures** included
- **Equations** correct (symbols and sub/superscripts)

Corrections should be made directly in the PDF file using the PDF annotation tools. If you have questions about this, please contact the editorial office. The corrected PDF and any accompanying files should be uploaded to the journal's Editorial Manager site.

Author Query Form

WILEY

Journal ADFM

Article adfm201800793

Dear Author,

During the copyediting of your manuscript the following queries arose.

Please refer to the query reference callout numbers in the page proofs and respond to each by marking the necessary comments using the PDF annotation tools.

Please remember illegible or unclear comments and corrections may delay publication.

Many thanks for your assistance.

Query No.	Description	Remarks
Q1	Please provide TOC keyword.	
Q2	Please confirm that forenames/given names (blue) and surnames/family names (vermilion) have been identified correctly.	
Q3	Please provide the highest academic title (either Dr. or Prof.) for all authors, where applicable.	
Q4	Please define EGDMA at first occurrence in the text.	
Q5	Please verify the inserted missing elements for correctness throughout the reference list.	
Q6	Please provide the page number for refs. 12a, 14a, if applicable.	

Author: Please confirm that Funding Information has been identified correctly.

Please confirm that the funding sponsor list below was correctly extracted from your article: that it includes all funders and that the text has been matched to the correct FundRef Registry organization names. If a name was not found in the FundRef registry, it may not be the canonical name form, it may be a program name rather than an organization name, or it may be an organization not yet included in FundRef Registry. If you know of another name form or a parent organization name for a "not found" item on this list below, please share that information.

FundRef Name	FundRef Organization Name
National Natural Science Foundation	National Natural Science Foundation of China
National Natural Science Funds for Distinguished Young Scholar	
National Key R&D Program of China	
China Scholarship Council (CSC)	China Scholarship Council
111 project	

Q1 xxxx

T. Zhao, G. Wang, D. Hao, L. Chen, K. Liu,* M. Liu* 1800793

Macroscopic Layered Organogel–Hydrogel Hybrids with Controllable Wetting and Swelling Performance

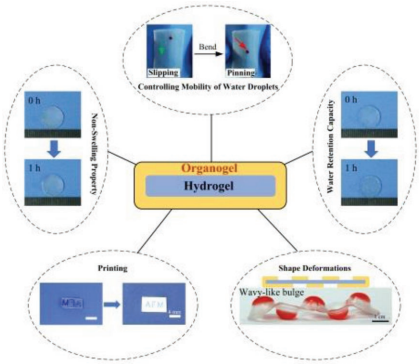

A simple yet versatile method is proposed to fabricate an organogel–hydrogel hybrid. The unique property of being externally hydrophobic and internally hydrophilic enables the organogel–hydrogel hybrid to exhibit a variety of functions, such as robust mechanical properties, long-lasting antiswelling and antidehydration, controlling mobility of water droplets, laser-assistant printing, and dimensional shape transformation.

Macroscopic Layered Organogel–Hydrogel Hybrids with Controllable Wetting and Swelling Performance

Tianyi Zhao, Guangyan Wang, Dezhao Hao, Lie Chen, Kesong Liu,* and Mingjie Liu*

Soft gels that integrate the water retention of hydrogels and the water swelling resistance of organogels are sought by researchers. Such materials have useful properties and potential applications in stretchable and biointegrated fields, such as tissue engineering, microfluidics, and biomedical devices. This study reports a simple yet versatile method for assembling hydrogels and organogels into covalently tethered hybrids to provide robust properties, such as excellent stretchability, tough interfacial bonds, enduring antiswelling, and low dehydration. The proposed method is simple and can generally be applied to hydrogels that contain hydroxyl terminal groups and commonly used organogels that can copolymerize with double-bond groups. The unique property of being externally hydrophobic and internally hydrophilic enables the organogel–hydrogel hybrids to be applied to many fields, such as mobility control of water droplets, printing, and 3D structure development. The organogel hydrogel hybrids not only present superior wettability performances, such as water retention and swelling resistance, but also present applicable functions that make them useful in tissue engineering and biomedical devices in vivo.

1. Introduction

Soft and flexible hydrogels with high water contents show promise for use as implantable or wearable biomaterials. Potential applications include artificial skin,[1] tissue engineering,[2] contact lenses,[3] drug delivery,[4] and in vivo biosensors.[5] Although remarkable progress has been achieved in the development of special hydrogels in recent decades,[6] their practical applications are limited by swelling and dehydration, which can drastically affect their mechanical toughness and other intrinsic properties.[7] Accordingly, there is an urgent need for nonswelling, dehydration-controlled hydrogels.[8] A lot of effort has been devoted to improve the swelling and dehydration properties of hydrogels. By utilizing physical or chemical methods, significant progress has been achieved.[9] For example, by physically adding highly hydratable salts to polyacrylamide hydrogel, more free water can be converted to bound water, thereby increasing the water retention capacity;[10] or, by complex chemical modification, different phases can be integrated from the intersurface to synthesize hydrogel–elastomer hybrids with multifunctional properties including extremely robust interfaces, low dehydration, and high elasticity.[1a] However, some intrinsic drawbacks in these techniques have been recognized: i) physical addition of materials may affect the inherent properties of the hydrogels;[11] and ii) chemical processes may be complex, requiring investigation via complicated experiments. Since these problems are critical in both practical applications and theoretical research, there is a pressing need to fabricate extremely robust hydrogels, especially those with optimal water retention, antiswelling, and elastic properties.[12]

Recently, building binary cooperative complementary materials with two components of entirely opposite physiochemical properties has been widely used and considered as a novel principle for the design of functional materials.[13] So far, hydrogels and organogels have been widely used in technological applications.[14] Because of the complementary wettability performances of hydrogel and organogel, they are expected to be integrated to provide even better performance in new applications.[15] For example, Gao et al. synthesized hydrophilic/oleophilic heteronetworks to mimic biological organisms with exceptional freezing tolerance.[14b] Such hydrophilic/oleophilic heteronetworks showed self-adaptive properties in different dispersion media, which appealed us to combine organogel and hydrogel to realize the resistance of swelling. Similarly, the surfaces of vegetables and fruits have thick epicuticular waxy layers to create a barrier to mass transfer, greatly slower the

Prof. T. Zhao, G. Wang, L. Chen, Prof. K. Liu, Prof. M. Liu
Key Laboratory of Bio-inspired Smart Interfacial Science and Technology of Ministry of Education
School of Chemistry
Beihang University
Beijing 100191, P. R. China
E-mail: liuks@buaa.edu.cn; liumj@buaa.edu.cn
D. Hao
Technical Institute of Physics and Chemistry
Chinese Academy of Sciences
Beijing 100190, P. R. China
D. Hao
School of Future Technology
University of Chinese Academy of Science
Beijing 100049, P. R. China
Prof. K. Liu, Prof. M. Liu
Beijing Advanced Innovation Center for Biomedical Engineering
Beihang University
Beijing 100191, P. R. China
Prof. M. Liu
International Research Institute for Multidisciplinary Science
Beihang University
Beijing 100191, P. R. China
The ORCID identification number(s) for the author(s) of this article can be found under https://doi.org/10.1002/adfm.201800793.

DOI: 10.1002/adfm.201800793

rate of water evaporation (drying), and maintain freshness.[10] Inspired by these observations from nature, researchers are aiming to improve the water retention and antiswelling properties of hydrogels by grafting hydrophobic compounds onto their surfaces. For example, Kamata et al. reported a nonswellable hydrogel by introducing hydrophobic thermoresponsive segments into a hydrophilic hydrogel polymer network.[8b] Meanwhile, Yao et al. presented a strategy to superhydrophobize a hydrogel surface by modifying hydrophobic groups or polymers. The introduction of hydrophobic compounds has improved the properties of hydrogels in various ways; however, there is still great potential for reducing swelling and increasing water retention. Achieving both at the same time would be especially valuable.

In this work, we aim to design a hydrogel that is covered by a hydrophobic, elastic organogel layer, to maintain the high water content, porosity, and soft consistency of the hydrogel, as well as the hydrophobic and swell repellency of the organogel. Although there are a few reports that organogels can be successfully attached to hydrogel surfaces by direct copolymerization of layered prepolymer, or rapid adhesion based on dynamic covalency, challenges still remain, such as building proper structures to achieve water retention and nonswelling of hydrogels simultaneously in practical application. Herein, we report a simple yet versatile strategy for coating synthetic hydrogels with organogels, creating organogel–hydrogel hybrids with extremely robust properties. By successively introducing double bonds onto a hydrogel surface, organogel–hydrogel hybrids were obtained by copolymerizing organogel monomers with the double bond groups. As the fabrication process is quite simple, this method can be widely applied to a diverse range of commonly used organogels and tough hydrogels. The as-prepared organogel–hydrogel hybrids address the previously mentioned challenges, as they achieve excellent antiswelling and long-lasting water retention properties simultaneously, with the additional properties of being semitransparent and elastic. The prepared hybrids also exhibit reversible control of the mobility of water droplet and light transmission changes. In addition, with the combined internal water absorption and the external water resistance, the prepared hybrids have potential practical applications in printing, liquid motion control, and 2D to 3D transformation. The current study not only presents a simple and versatile method for the large-scale manufacture of robust organogel–hydrogel hybrids, but also proposes applicable functions such as printing and dimensional transformations, which may shed light on preparing biomedical devices.

2. Results and Discussion

2.1. Fabrication of Organogel–Hydrogel Hybrids

Although organogels and hydrogels are used separately in many technological applications, there is still an urgent need for organogel–hydrogel hybrids because of their complementary wettability performance. Herein, we developed a simple method for fabricating organogel–hydrogel hybrids. The essential ideas are i) introduction of double bonds onto the hydrogel surface, to act as anchoring points for organogel copolymerization; ii) cross-linking copolymerization of the immobilized double bonds and organogel monomers. The detailed procedures are shown in **Figure 1**. Figure 1a,b presents the hydrogel components and organogel components, respectively. Here, 2-hydroxyethyl acrylate (HEA) is chosen as the hydrogel monomer that

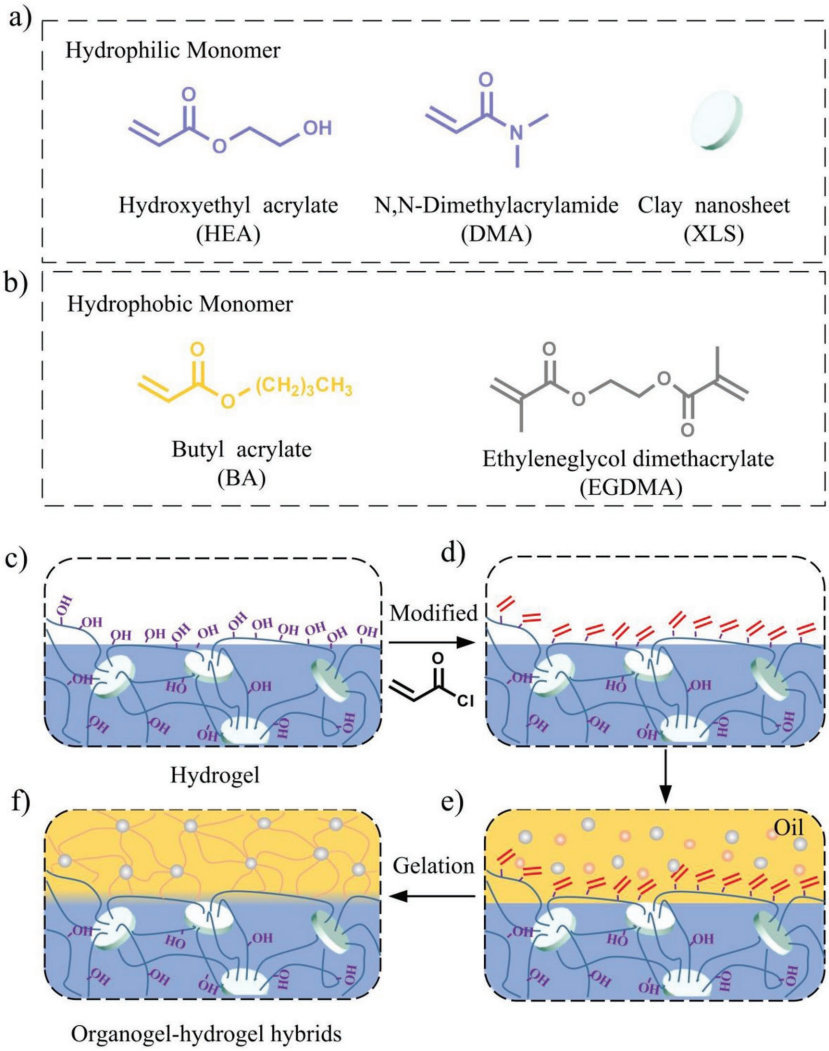

Figure 1. Fabrication processes of organogel–hydrogel hybrids. a) The hydrogel components: common monomers, DMA, and clay nanosheets. b) The organogel components: common monomers (in orange ball) and cross-linking agent EGDMA (in gray). c–f) Preparation of organogel onto hydrogel surface: c,d) by reacting with acryloyl chloride, double bonds are introduced onto the hydrogel surface; e,f) organogel layer is prepared on the hydrogel surface by copolymerizing the organogel monomers with the double bonds.

provides hydroxyl terminal groups as surface grafting sites for postgelation, and clay nanosheets (Laponite XLS) are used as the physical cross-linkers. The hydrogel is prepared by copolymerizing N,N-dimethylacrylamide (DMA) with HEA. Then, by reaction with hydroxyl groups on the HEA (Figure S1, Supporting Information), double bonds can be successfully introduced onto the hydrogel surface (Figure 1c,d). The presence of double bonds was confirmed in the infrared spectra (Figure S2, Supporting Information). The peaks at 3000 cm^{-1} were identified as characteristics peaks of H—C=, which indicates that double bonds were successfully grafted onto the hydrogel. Subsequently, the double bond-terminated hydrogel was immersed in paraffin oil containing organogel monomers, a cross-linking agent, and a photoinitiator to fabricate the organogel layer (Figure 1e,f). Due to the high water content (70–90 wt%) of the hydrogel, oil cannot penetrate it; therefore, the target functional entities (such as the organogel monomers) can be confined solely to the hydrogel surface. Finally, with the organogel monomers copolymerizing with each other and reacting with the double bonds, an organogel layer was formed and grafted onto the hydrogel surface (Figure 1f). Infrared spectrum was examined to test the modification state of organogel on hydrogel surface. As shown in Figure S2 (Supporting Information), the peaks at 3000 cm^{-1} (—C=H) of hydrogel sample were replaced by 2958 cm^{-1} ($-CH_3$) on hybrid sample, and the peaks at 3380 cm^{-1} (—OH) were disappeared on hybrid sample, can prove the surface grafting of organogel onto the hybrogel surface. In general, this reaction pathway is drastic, straightforward, and can be carried out under an ambient atmosphere without requiring an inert gas system. Furthermore, this approach has no particular requirement for the organogel monomer. Hence, almost all organogel monomers that can copolymerize with double bond groups are all suitable. In this work, we tried three different organogel monomers: butyl acrylate (BA), lauryl methacrylate (LMA), and methyl methacrylate (MMA), all of which were successfully synthesized onto a hydrogel surface (see Figure S4a, Supporting Information, for the chemical structures of LMA and MMA). Meanwhile, most hydrogels that contain hydroxyl as their terminal functional groups can be used. In this way, a variety of organogel-coated hydrogels can be fabricated according to different assemblies of hydrogel base and organogel monomers. Although hybrids with different organogel and hydrogel compositions can be produced by this strategy, this paper focuses on the properties of butyl acrylate-covered hydrogel (H-BA) as an example. Such a simple and versatile fabrication approach may broaden the application potential of hydrogels.

In addition, it was found that the thickness of the organogel layer can be precisely controlled during the polymerization process of the organogel precursor. With artificial control of the distance between the hydrogel surface and the coverslip, the thickness of the organogel layer was varied from 20 to over 600 μm (Figure S3, Supporting Information). With controllable thickness of the organogel layer, the as-prepared hydrophobic organogel–hydrogel hybrids will have wide practical applications. Compared with the hydrogel layer, the modified organogel layer was expected to provide different wetting properties and surface morphology.

2.2. Wettability Performance of Organogel–Hydrogel Hybrids

2.2.1. Contact Angle of Organogel–Hydrogel Hybrids

Special wettability on hydrogel surfaces has been desired for a long time because of its usefulness in anti-biofouling,[16] contact lenses,[17] etc. The hybrid produced in this study exhibited special wettability performance. Water contact angle (CA) is a convenient way to evaluate the wettability properties of surfaces. As shown in **Figure 2**a, the pristine hydrogel had a superhydrophilic CA of about 0° that increased to 86° after BA organogel was copolymerized onto it. Similarly, other organogel–hydrogel hybrids, such as H-BA + LMA (butyl acrylate and lauryl methacrylate cocovered hydrogel), H-BA + MMA (butyl acrylate and methyl methacrylate cocovered hydrogel), and H-LMA (lauryl methacrylate-covered hydrogel) demonstrated CAs of 80.1°, 85.6°, and 94.6°, respectively (Figure S4b, Supporting Information). In this case, according to the new hydrophilic/hydrophobic boundaries,[18] the modified hydrogel surface that contains the organogel layers are hydrophobic surfaces. Such hydrophobic performance was attributed to the low surface energy of the organogels, which further demonstrated that the process of modifying hydrophobic entities onto hydrogel surfaces is quite successful.[19] The stabilities of wettability performances are

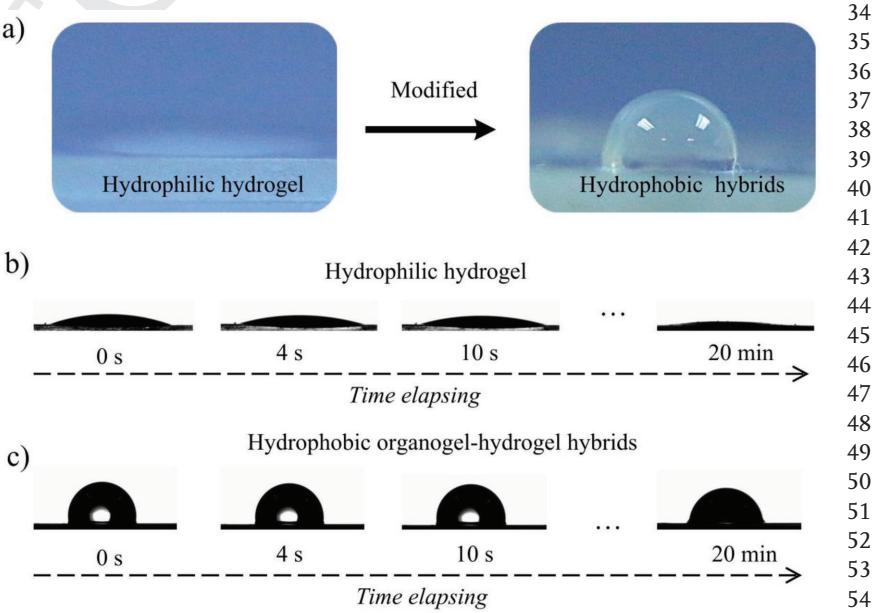

Figure 2. Wettability performance of the pure hydrogel and the organogel–hydrogel hybrid. a) Photographs of a water droplet deposited on hydrogels before (left) and after (right) organogel modification. b) A series of snapshots recording CA value changes within 20 min on the pure hydrogel surface. c) A series of snapshots recording CA value changes within 20 min on the organogel–hydrogel hybrid surface.

also examined by measuring the time-dependant CAs on the surfaces of both the hydrogel and organogel–hydrogel hybrids within 20 min. As shown in Figure S5 (Supporting Information), CA decreased quickly in the hydrogel surface within about 3 min; while on the hybrid surface, the CA decreased from 105° to 90° within the first 3 min but slightly decreased to 80° during the remaining 17 min. The CA changes on hybrid surface can be mainly attributed to two factors. First, the lubricant organogel surface makes the water droplet need time to spread and form a stable three-phase contact line, which causes the decrease of CA from 105° to 90° within the first 3 min. On the other hand, with the extension of time, evaporation is the main reason of CA decrease, which causes the slight decreasing of the CA. As shown in Figure 2b,c, the stability of the wettability performances can be proved on organogel–hydrogel hybrid surface.

2.2.2. Controlling Mobility of Water Droplets on the Hybrid Surface

Adjusting fluidity is an interesting area of study for surface wettability control.[20] Dynamically manipulating the mobility of water droplets on the surface can be realized by continuous tuning of the film's morphology.[21] By using soft solid materials as substrates, for example, hydrogels, there are further possibilities for controlling fluids due to their superelastic properties, which can directly lead to topomorphological changes. The organogel–hydrogel hybrid prepared in this work has excellent elasticity, which can induce surface geometry changes by bending and thus further controlling the fluid mobility. After dropping silicon oil onto the hybrid's surface, the silicon oil spread over and covered the whole surface to form an oil-infused elastic solid. The silicon oil on the surface of the organogel layer serves as a lubricating layer that allows water droplets to slide easily. However, the sliding mobility will be changed when applying a force to bend the sample (**Figure 3**a). Figure 3b demonstrates the sliding mobility of a water droplet on an undeformed substrate in which the droplet slides down the surface freely in about 2 s. Figure 3c shows the transformation between different mobility modes. The water droplet also slides down the relaxed hybrid surface in the initial stage but, when bending the sample, the sliding water droplet slows down and stops when the membrane is bent (Figure 3ci–v). In addition, the sliding of water droplets can be recovered after the stress is released, which means that the adjustment of mobility can be continuously cycled by repeating the bending and

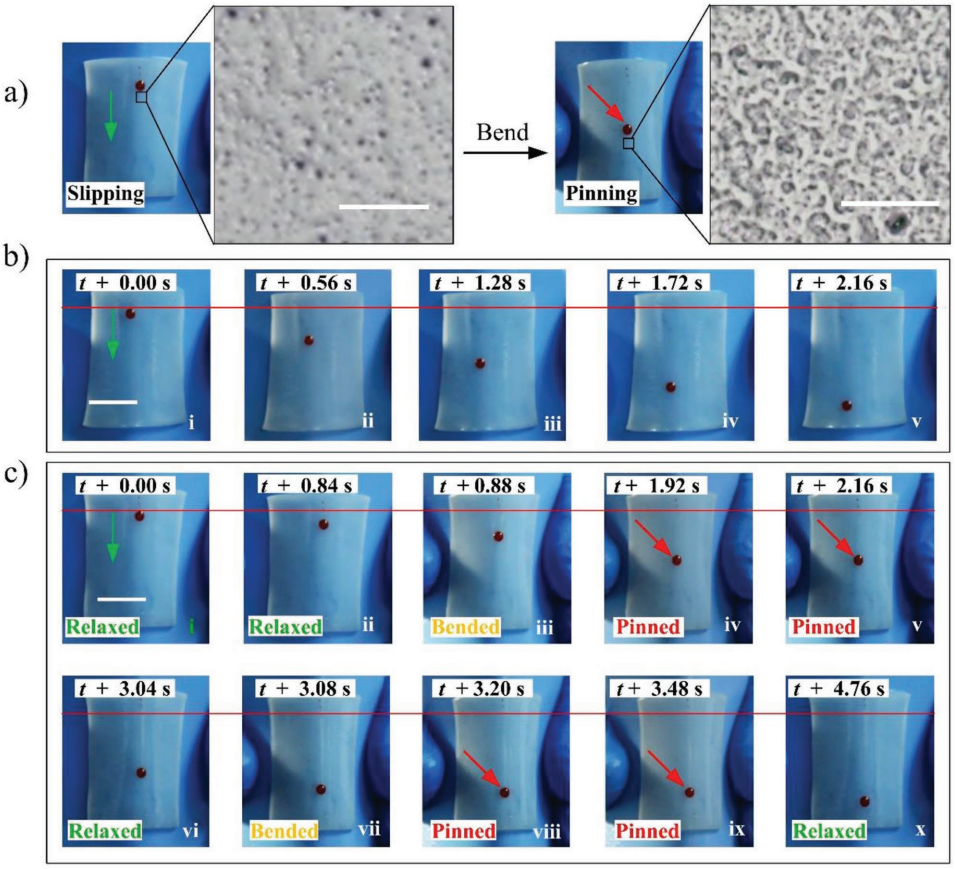

Figure 3. Dynamic control of water droplet mobility. a) The water droplet slides down the hybrid surface when the hybrid is in a relaxed state, while the water droplet is pinned firmly onto the surface when the hybrid is bending. The augmented pictures show the detailed structure of the hybrid surface, where the microscale roughness is increased while bending. Scale bars = 100 µm. b) Images of water droplets sliding off the hybrid surface. Scale bars = 1 cm. c) The mobility shifts between sliding and pinning by relaxing and bending the hybrid. Scale bars = 1 cm.

releasing (Figure 3cvi–x). Comparing the topomorphologies of the substrate in the undeformed and bent states (Figure 3a), the microscale structure was enlarged when the organogel layer was stretched, at the same time the surface of the oil is decreasing, which finally affects the droplet sliding on the surface. Basically, the upper organogel layer is a 3D network of polymer chains on the surface. Such 3D structures are deformed into larger sizes during the stretching process, causing them to firmly anchor the water droplet at the surface. The 3D structures can be attributed to the precipitation polymerization, as the organogel is insoluble in paraffin oil and thus precipitates to create microstructures. Furthermore, as the 3D network of the organogel layer prepared in this work is in microscale/nanoscale, plays the role of storage of oil, the mobility control of tiny water droplet (1 µL) can be realized. Therefore, due to changes in the surface structure during stretching, the material provides a simple and stimulus-responsive method to tune water droplet mobility. Meanwhile, this transition from a smooth to a rough surface also causes light transmission changes. The infused organogel membrane turns from translucent into opaque while bending (Figure S6, Supporting Information). The reason would probably be attributed to the redistribution of silicon oil on the augment 3D network of organogel and the partially filled network was filled with air, which effectively reduces the light scattering at the surface/air interface. Therefore, other than mobility of water droplets, the film's optical transparency can also be adjusted by relaxing or bending the hybrid.

2.2.3. Augmenting the Hydrophobicity by Stretching the Hybrids

In addition to the long-term stable hydrophobicity mentioned above, the organogel–hydrogel hybrids also exhibit sustained hydrophobicity during stretching (Figure S7a, Supporting Information). As hydrogel–elastomer hybrids are liable to be used in stretching conditions, we conducted CA measurements on stretching organogel–hydrogel hybrids. The as-prepared organogel–hydrogel hybrids showed constant hydrophobic CAs and intact surfaces throughout the entire stretching process; in addition, the CAs significantly increased from about 100.6° to 110.0° after the material was stretched by 300% (**Figure 4**a,b). This hydrophobic shift could also be attributed to morphological changes during stretching (Figure S7b, Supporting Information). When stretching the hybrid to 50% deformation, significant microscale structure emerged (comparing with the original state), which can trap more air at the surface and stimulate increased hydrophobic performance. However, further stretching cannot arouse more CA augment, because the surface structure changing is not significant enough to change the CA value.

2.3. Robustness of Organogel–Hydrogel Hybrids

2.3.1. Mechanical Robustness of Organogel–Hydrogel Hybrids

The continuous coverage of the organogel layer on the hydrogel surface provides robustness, which can be demonstrated

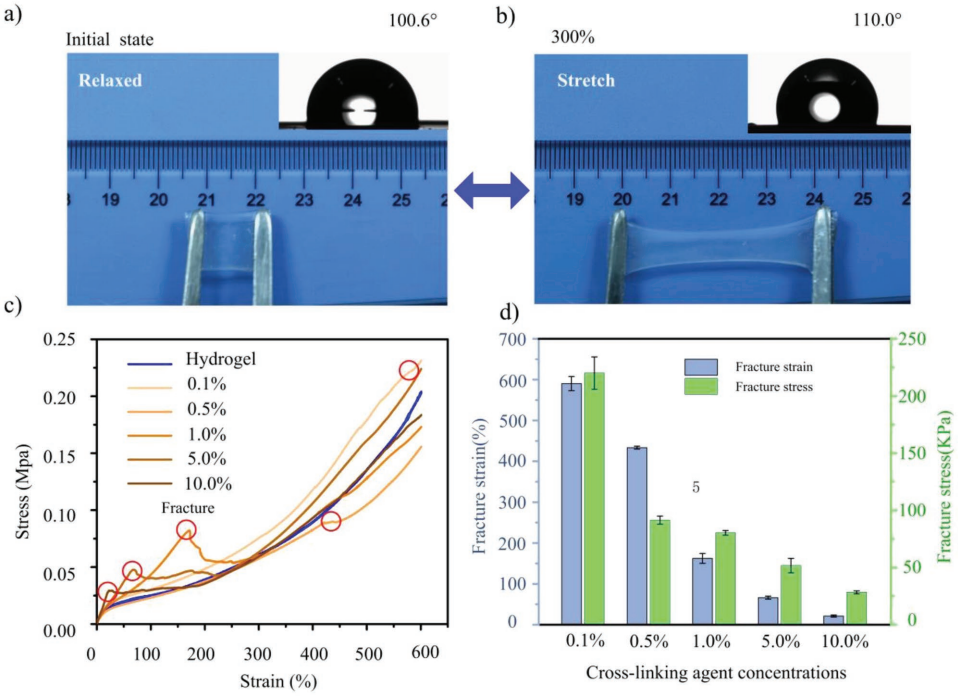

Figure 4. Wettability and mechanical properties of the organogel–hydrogel hybrid during stretching. a) The hydrophobic performance of the organogel–hydrogel hybrid in its initial state. b) The increased hydrophobic performance of the organogel–hydrogel hybrid in the 300% stretching state. c) Stress–strain curves of pure hydrogel and the organogel–hydrogel hybrids with different cross-linking agent concentrations. The percentages represent the cross-linking agent used during the formation of the organogel layers. The peaks circled in red are the break-points of the organogel layer. d) The fracture strain and fracture stress of the organogel–hydrogel hybrids with different cross-linking agent concentrations (the transverse ordinates of the fractured points in the Figure 4c).

during deformation. In fact, after acetone and acid chloride treatment, the mechanical properties of the hydrogel are increased, because the dehydration leads to the expose of polymer network, which increases the fracture stress and fracture strain. Figure 4c shows the 600% stretching stress–strain curves for all kinds of hydrogel samples. This facilitates evaluation of the fracturing properties of organogel–hydrogel hybrids, as well as the interfacial toughness of organogels bonded on hydrogel substrates. The peaks on stress–strain curves (circled in red in Figure 4c) represent the fracture of the organogel layer. It can be observed that the hydrogel layer did not fracture during such a high amount of stretching, but organogel layers were fractured and its tensile strength was greatly reduced by increasing the concentration of cross-linking agents. For better comparison, the detailed fracture stress and the fracture strain of the organogel layers with different cross-linking agent concentrations are shown in Figure 4d. As the cross-linking agent increases, the hybrid becomes more brittle, so the elongation at break and the fracture strength are relatively low. However, according to the actual fractured situation of the hybrids, the organogel layer did not peel off from the hydrogel surface, indicating that the organogel–hydrogel interface remains intact without debonding during the entire stretching test, even after fracture of the organogel layer, which demonstrates the robustness of organogel–hydrogel interfacial bonds. According to our experiments, in order to obtain high quality mechanical properties as well as robust interfacial bonds, the concentration of the cross-linking agent should be controlled within a low range. Indeed, when using a concentration of cross-linking agent that is within the optimal range (≈0.1–0.5 wt%), the as-prepared organogel–hydrogel hybrids exhibit excellent mechanical properties, with high tensile strength and maximum stretchable deformation of more than 300%. We studied the stretching cycle of H-0.5%BA (H-BA hybrid with 0.5 wt% cross-linking agent; similar notation is used for other hybrids) in detail. Samples were stretched 300%, and then allowed to return to their original size. Digital and optical microscopy images (Figure 4a,b) show that this stretching cycle can be conducted without causing any obvious damage to the surface. Therefore, the as-prepared organogel–hydrogel hybrids exhibit robust properties such as high mechanical strength, robust interfacial bonds, and reusability.

2.3.2. Nonswelling Property of Organogel–Hydrogel Hybrids

The robust organogel–hydrogel hybrid we created has properties that exceed those of pure hydrogel or organogel systems, prompting us to further explore its excellent properties and potential applications. Covered by a tough organogel layer, the hydrophilic performance of the hydrogel layer can be largely protected to achieve super-stable properties such as nonswelling (a schematic illustration of the mechanism is shown in **Figure 5**a). Accordingly, nonswelling tests were carried out by immersing hydrogels in deionized water for a certain time and measuring changes in their mass. During the swelling process, the samples' morphological changes were recorded by a digital camera. After swelling for 24 h, the volume of the pure hydrogel substrate increased greatly, while the organogel–hydrogel substrate remained almost the same (Figure 5b). The swelling ratio was accurately calculated by measuring the mass of the samples regularly by Equation (1) (Supporting Information), and the experiment was prolonged to 7 d duration (168 h). The pure hydrogel substrate swelled to its maximum swelling ratio of ≈350% within 12 h (Figure 5c). Meanwhile, the organogel–hydrogel substrates remained at a very low swelling ratio after immersion in water for 7 d. This excellent nonswelling property provides the as-prepared organogel–hydrogel strong repellency in water systems, which could be useful for in vivo applications.

2.3.3. Water Retention Capacity of Organogel–Hydrogel Hybrids

Similarly, the construction of organogel-covered hydrogel mimics mammalian skin or waxy layer of plant leaves, in which the epidermis protects the body from dehydration (as schemed in Figure 5d). Therefore, water retention capacity tests were carried out by keeping the samples in a chamber with 10% relative humidity (RH) at 22 °C. The morphological changes in the samples were recorded by a digital camera. After 48 h of dehydration, pure hydrogel shrunk greatly and became stiff; whereas organogel-covered hydrogel only shrunk slightly and maintained an elastic surface (Figure 5e). This indicates that water evaporates much more slowly in the organogel–hydrogel hybrid system. To accurately evaluate the water loss of the hydrogel samples, their masses were recorded at time intervals using an electronic scale. Figure 5f shows the dehydration ratio (calculated by the Equation (2), Supporting Information) over time for pure hydrogel and organogel–hydrogel hybrids with various concentrations of cross-linking agent. The samples were also kept in a chamber at 10% RH and 22 °C, and the experiment time was prolonged to 7d (168 h). With time, all hydrogels exhibited dehydration to various degrees. Water loss occurred at a gradually increasing rate and then reached a steady-state threshold where no more water evaporated. The pure hydrogel lost water dramatically and reached its threshold at 12 h, with dehydration of more than 60%. By contrast, the organogel–hydrogel hybrids exhibited a very low rate of water loss within the first 96 h which remained nearly the same until the end of the experiment (168 h), with total dehydration of less than 15%. However, there were no serious differences between organogel–hydrogel hybrids prepared with various cross-linking agent concentrations. As the water retention threshold was reached at about 96 h, it is believed that a high ratio of water (more than 85%) will be retained by organogel–hydrogel hybrids indefinitely. Therefore, with an organogel coating, the water retention capacities of hydrogels can be greatly improved and their dehydration ratios maintained at very low levels. Thus, the organogel coating not only affords hydrogels a nonswelling ability, but also an excellent water retention capacity.

As all the organogel–hydrogel hybrids exhibited high water retention and good nonswelling qualities irrespective of the cross-linking agent concentrations, the organogel covering is the crucial aspect of these special properties. In a hydrogel, water molecules are distributed equally in the interior and on the surface, and are free to transfer between the hydrogel and the external environment. However, in hydrogels with

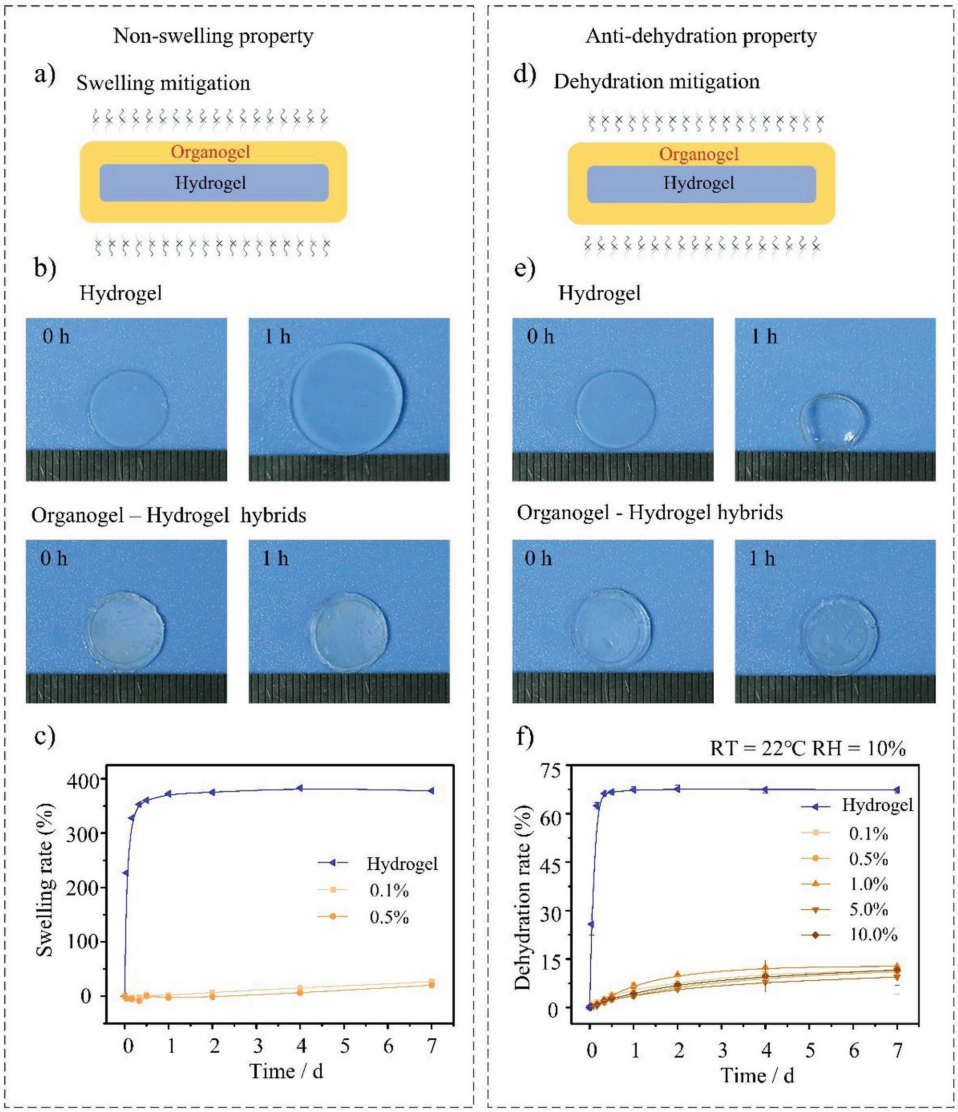

Figure 5. Antiswelling and water retention of the organogel–hydrogel hybrid. a,d) Schematic illustration of the antidehydration and water retention of the hybrid. An organogel layer robustly bonded to the hydrogel can effectively prevent water penetration into or evaporation from the hydrogel. b) Snapshots of hydrogel and the organogel–hydrogel hybrid taken at the initial time and after being immersed in water for 24 h. e) Snapshots of hydrogel and the organogel–hydrogel hybrid taken at the initial time and after being naturally dehydrated under the ambient testing conditions (10% RH and 22 °C) for 24 h. The organogel–hydrogel hybrid does not show any significant change after 24 h of immersion or dehydration, whereas pure hydrogel shows noticeable changes after being immersed in water or naturally dehydrated for 24 h. c,f) When the testing time was prolonged to 7 d, the organogel–hydrogel hybrid still shows weight change less than 15% while the hydrogel without an organogel coating swells by more than 300% or shrinks by more than 60% of its original weight.

organogel coatings, the organogel layer tightly wraps the hydrogel, forming a barrier to water transfer (as illustrated in Figure 5a,d). Although the organogel-coated hydrogel maintains the same semitransparent and flexible properties as uncoated hydrogel, the organogel layer provides protection against dehydration.

2.4. Printing Application of Laser-Etched Hybrids

According to their nonswelling and water retaining properties, organogel–hydrogel hybrids are substrates with excellent internal hydrophilic and external hydrophobic characteristics. To demonstrate this by experiment, we compared samples of pure hydrogel with the organogel–hydrogel hybrid by painting water-soluble ink evenly onto their surfaces. With pure hydrogel, the ink was absorbed and covered the entire surface quickly (**Figure 6**a). By contrast, the organogel–hydrogel hybrid showed outstanding liquid resistance, with the ink droplet completely washing of the surface (Figure 6b). Therefore, the inner part of the hybrid, composed of pure hydrogel, can absorb water easily, while the external organogel layer prevents water from entering. Such extreme inner hydrophilicity and excellent outer hydrophobicity enables these organogel–hydrogel hybrids

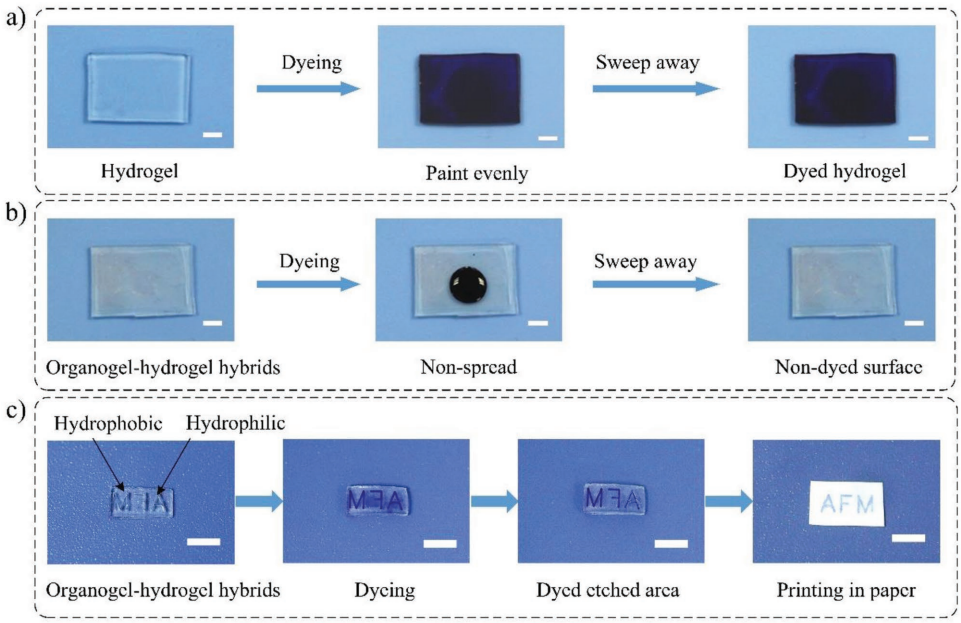

Figure 6. Different dyeing absorption performances of the hydrogel and the organogel–hydrogel hybrid, and the printing application. a) Water-soluble dyes can be absorbed and cover the entire pure hydrogel surface quickly. b) The water-soluble dyes can be completely washed from the surface of the organogel–hydrogel hybrids. c) The printing process of the as-prepared organogel–hydrogel hybrids. The organogel–hydrogel hybrid was treated by laser to fabricate special characters (for example, AFM) on the surface. After laser treatment, the organogel layer is etched off, resulting in the hydrophilic hydrogel being exposed on the surface. Water-soluble dyes (ink, for example) were dropped onto the surface and absorbed quickly by the hydrophilic etching area, but the nonetching area showed resistance of dyeing because of its hydrophobic organogel layer. The ink absorbed by the organogel–hydrogel hybrid was further pressed on paper and showed the characters successfully. Scale bars = 4 mm.

to be used as printing templates (Figure 6c). In addition, by laser etching, the organogel layer can also be remodified to achieve efficient reusability of the substrate. The printing experiment is just one example of a potential application for our organogel–hydrogel hybrids, which will undoubtedly prompt many innovations.

2.5. Shape Deformation of Organogel–Hydrogel Hybrids

According to the different swelling ratios of the organogel and the hydrogel, the structure can be transformed from 2D to 3D. A bilayer organogel–hydrogel hybrid consisting of one layer of hydrogel and one layer of organogel was fabricated. When the bilayer hybrid was immersed in dyed water, the hydrogel layer absorbed a large amount of water, leading to a significant volume expansion, whereas the organogel layer remained almost its original volume (**Figure 7**a). Thus, the bilayer hybrid became curved due to the nonuniform stress distribution of the binary cooperative complementary effect of the hydrogel and the organogel networks (Figure 7b). Based on this principle, complicated shapes can be fabricated. For example, when the bilayer hybrid is tailored into a flower shape, a flower bud structure is obtained after swelling (Figure 7c). When the hydrogel layer is cut into a flower shape while the organogel layer remains a circle, a blooming flower structure is obtained after swelling (Figure 7d). With the concept of organogel–hydrogel bilayer hybrid, complex 3D deformations, such as combination structures of bending/unbending and expansion/contraction, can be achieved simply by controlling the area or the shape of hydrogel or organogel layers.

To organogel fully covered hydrogel, laser is used as an assistance to etch patterns on hybrids. With laser etching, the hybrid can be etched into two regions: the etched region with the hydrogel exposed on the surface and the unetched portion that is covered by the organogel. When the etched hybrid is immersed in water, the etched and unetched regions show different swelling/nonswelling properties, causing an in-plane stress that can drive shape deformations from a 2D flat film into a 3D structure (Figure 7e). By etching a circle pattern on the hybrid, we can obtain a cap-like buldge on top of the hybrid (Figure 7f). Also, when we etched circles onto both sides of the hybrid surface alternately, wavy-like buldges can be obtained (Figure 7g). Sophisticated 3D deformations can also be achieved by control the etching area or the shape of organogel layers. Because of the different hydrophobic and hydrophilic regions of the hybrids formed by laser etching technique, it is assumed that the deformation rate and degree of the hydrogels can be precisely adjusted. In this case, with purposeful design of the etching architecture, the swelling/nonswelling regions of the hybrid could be precisely controlled to develop a programmable shape of deformations.

3. Conclusion

In this work, we presented a facile and versatile method of fabricating organogel-covered hydrogels with robust properties, merely by copolymerizing organogel monomers with

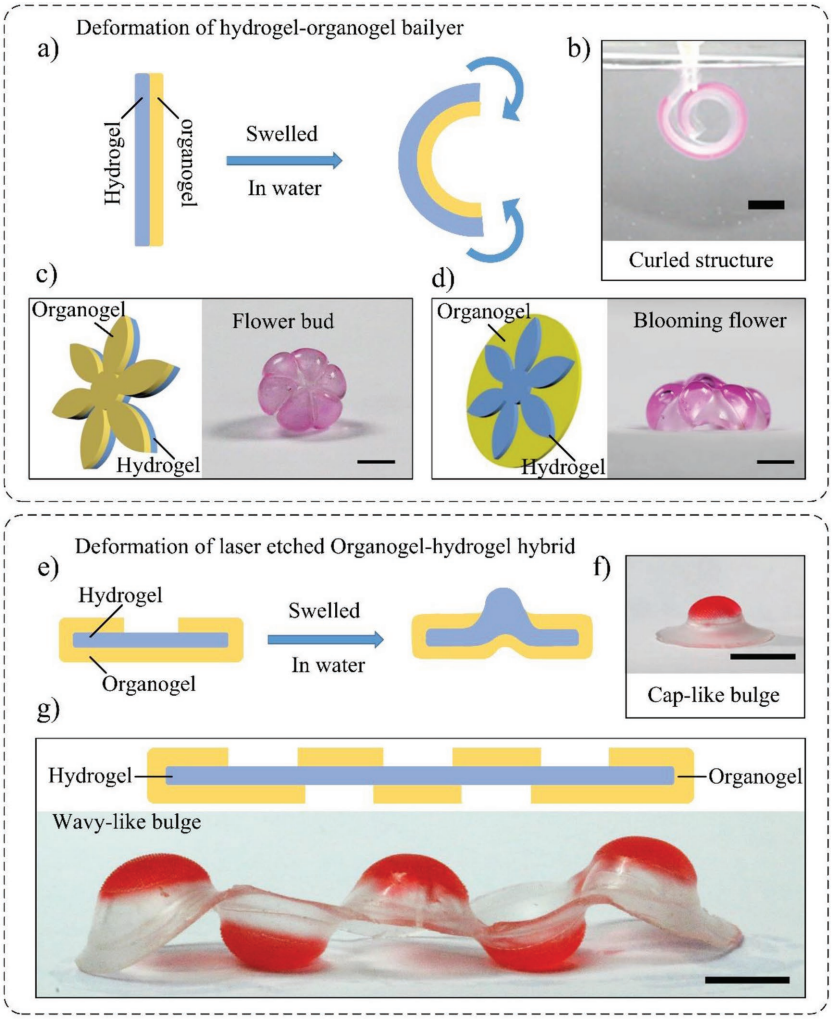

Figure 7. Shape deformation from the 2D laser-etched organogel–hydrogel hybrids to complex 3D structures. a) The schematics of the deformation mechanism of the bilayer organogel–hydrogel hybrid. b) The bilayer organogel–hydrogel hybrid gradually deformed into a curved structure when swelling in water. c) A flower bud structure that deformed from flower shaped bilayer hybrid. d) A blooming flower structure deformed from the bilayer hybrid which composed of the flower shaped hydrogel layer and the circle shaped organogel layer. e) The schematics of the deformation mechanism of fully covered organogel–hydrogel hybrids. f) The hemispherical bulge structure deformed from organogel–hydrogel hybrid with circle pattern etched on the surface. g) 3D shapes formed from the hybrid with circle patterns etched on both sides of the surface alternately. Scale bars = 1 cm.

immobilized double bonds on the hydrogel surface. Most importantly, the proposed strategy does not rely on the special intrinsic wettability of monomers, which makes it applicable to an extensive range of hydrogels and organogels. The results demonstrated that sustainable hydrophobicity was achieved on the outer organogel surface while superhydrophilicity was retained inside. Therefore, the as-prepared organogel–hydrogel hybrids exhibited excellent antidehydration and water retention properties simultaneously. The potential applications such as printing and 2D to 3D deformation were used to demonstrate the advantages of the outer hydrophobicity/inner hydrophilicity of our organogel–hydrogel hybrid material. The simultaneous antiswelling/water retention properties of our robust organogel–hydrogel hybrids may prove useful in various applications, particularly in biomedical devices deployed in physiological environments, such as intravascular stent and tissue filling.

4. Experimental Section

Materials: HEA was purchased from Aladdin Ltd. (Shanghai, China). DMA, LMA, and acryloyl chloride were bought from J&K Chemical Ltd. 2,2-diethoxyacetophenone (DEOP), triethylamine, perylene red, and EGDMA were obtained from TCI (Shanghai, China). Acetone, ethyl acetate, and 1,2-dichloroethane were from the Beijing Chemical Reagent Co., Ltd. Paraffin oil was supplied by Sigma-Aldrich (Shanghai, China). Laponite XLS was purchased from Rockwood Ltd. BA was obtained from Sinopharm Group Chemical Reagent Co., Ltd. MMA was purchased from Alfa Aesar. All reagents were used as received. The water used throughout all experiments was purified through a Millipore system.

Preparation of Hydrogel: A typical precursor was as follows: HEA (4 wt% of the total solution), DMA (16 wt% of the total solution), and clay nanosheets (Laponite XLS; 7 wt% of the total solution) were dissolved in deionized water, then 0.5 wt% of the photoinitiator DEOP was added. Subsequently, the as-prepared precursor was stirred by a defoaming mixer to make sure all components were evenly dispersed. The stirred precursor was placed onto a clean glass plate and covered with a clean coverslip. The thickness between the glass plate and coverslip was controlled by adding 1 mm silicone gasket on both sides. Transparent hydrogel was obtained after UV irradiation (wavelength ≈ 365 nm) was applied for 10 min.

Modification of Acryloyl Chloride on Hydrogel: The hydrogel was first rinsed in acetone (CH_3COCH_3) to dehydrate it for 30 s, in order to avoid the vigorous reaction between acryloyl chloride and water. Then the hydrogel was immediately immersed in ethyl acetate with a certain amount of triethylamine, followed by addition of acryloyl chloride drop-wise under stirring (acryloylchloride:ethyl acetate ratio was 1:3 by volume). The hydrogel was rinsed with water and dried by nitrogen flow before further use.

Preparation of Organogel–Hydrogel Hybrids: The pregel solution was prepared by mixing organogel monomers (60 wt% of the total solution), cross-linking agent EGDMA (adjusted from 0.1, 0.5, 1, 5, and 10 wt% of the organogel monomers) and photoinitiator DEOP (0.2 wt% of the organogel monomers) into the solvent, paraffin oil (40 wt% of the total solution). The organogel monomers were varied between pure BA, a 1:1 mixture of BA and LMA, a 1:1 mixture of BA and MMA, and pure LMA. After placing the acryloyl chloride-modified hydrogel onto a clean coverslip, organogel pregel solution was added to the hydrogel, and then covered by a clean coverslip. The thickness between the two coverslips was also controlled by adding 1 mm silicone gaskets and slides on both sides. UV irradiation was applied for 15 min to complete the polymerization, and the organogel–hydrogel hybrids were prepared.

Water Contact Angle Measurement of Gel Surfaces: Water contact angles were measured on a video-based optical contact angle measuring system (OCA40 Micro, Dataphysics Instruments GmbH, Germany) at ambient temperature. The water droplets were all about 2 µL and placed

carefully onto the gels in the air. The average value of ≥5 measurements performed at different positions on the same sample was used as the contact angle.

Measurement of Organogel Layer Thickness: The fluorescent dye perylene red was used for staining the organogel layer. It was first dissolved in dichloromethane to form a solution of concentration 10^{-6} mol L^{-1}, then dripped onto the organogel–hydrogel hybrids. After complete evaporation of dichloromethane, the perylenered solution was dripped again. After 5 cycles of dripping and evaporation, the organogel–hydrogel hybrid was considered to be completely dyed. The dyed organogel–hydrogel hybrid sample was sectioned and the thickness of the dyed organogel layer was measured under a microscope.

Characterization: The chemical composition was analyzed by Fourier transform infrared spectroscopy (AVATAR360, Tianjin Gangdong SCI & Tech. Development Co. Ltd., China). The mechanical properties were measured by an electronic universal testing machine (UTM4103, Shenzhen SUNS Technology Stock Co. Ltd., China) at a stretching speed of 10 mm min^{-1}. Images were obtained with a digital SLR camera (Canon EOS70D). The laser was generated by a nanosecond pulse laser device (LSC20 CO2, Wuhan Huagong Laser Engineering Co. Ltd., China).

Supporting Information

Supporting Information is available from the Wiley Online Library or from the author.

Acknowledgements

T.Z. and G.W. contributed equally to this work. This work was supported by the National Natural Science Foundation (Grant No. 21574004), the National Natural Science Funds for Distinguished Young Scholar (Grant No. 21725401), the National Key R&D Program of China (Grant No. 2017YFA0207800), China Scholarship Council (CSC) Grant No. 201606025097, the 111 project (Grant No. B14009), the Fundamental Research Funds for the Central Universities, and the National 'Young Thousand Talents Program'.

Conflict of Interest

The authors declare no conflict of interest.

Keywords

nonswelling property and antidehydration property, organogel–hydrogel hybrids, printing, robustness, shape deformation

Received: January 31, 2018
Revised: April 28, 2018
Published online:

[1] a) H. Yuk, T. Zhang, G. A. Parada, X. Liu, X. Zhao, *Nat. Mater.* **2016**, *7*, 12028; b) Y. Wu, X. Pei, X. Wang, Y. Liang, W. Liu, F. Zhou, *NPG Asia Mater.* **2014**, *6*, e136.

[2] a) L. Li, Y. Wang, L. Pan, Y. Shi, W. Cheng, Y. Shi, G. Yu, *Nano Lett.* **2015**, *15*, 1146; b) S. Gnavi, L. Blasio, C. Tonda-Turo, A. Mancardi, L. Primo, G. Ciardelli, G. Gambarotta, S. Geuna, I. Perroteau, *J. Tissue Eng. Regener. Med.* **2017**, *11*, 459; c) K. Y. Lee, D. J. Mooney, *Chem. Rev.* **2001**, *101*, 1869.

[3] X. Hu, H. Tan, P. Chen, X. Wang, J. Pang, *J. Nanosci. Nanotechnol.* **2016**, *16*, 5480.

[4] a) S. Merino, C. Martín, K. Kostarelos, M. Prato, E. Vázquez, *ACS Nano* **2015**, *9*, 4686; b) J. Wu, A. Chen, M. Qin, R. Huang, G. Zhang, B. Xue, J. Wei, Y. Li, Y. Cao, W. Wang, *Nanoscale* **2015**, *7*, 1655; c) M. M. Pakulska, K. Vulic, R. Y. Tam, M. S. Shoichet, *Adv. Mater.* **2015**, *27*, 5002.

[5] a) J. Yuan, D. Wen, N. Gaponik, A. Eychmüller, *Angew. Chem.* **2013**, *125*, 1010; *Angew. Chem., Int. Ed. Engl.* **2013**, *52*, 976; b) L. Li, Y. Shi, L. Pan, Y. Shi, G. Yu, *J. Mater. Chem. B* **2015**, *3*, 2920.

[6] a) E. Bormashenko, Y. Bormashenko, A. Musin, Z. Barkay, *ChemPhysChem* **2009**, *10*, 654; b) P. Aussillous, D. Quere, *Nature* **2001**, *411*, 924; c) N. M. Oliveira, Y. S. Zhang, J. Ju, A.-Z. Chen, Y. Chen, S. R. Sonkusale, M. R. Dokmeci, R. L. Reis, J. F. Mano, A. Khademhosseini, *Chem. Mater.* **2016**, *28*, 3641.

[7] a) C. Keplinger, J.-Y. Sun, C. C. Foo, P. Rothemund, G. M. Whitesides, Z. Suo, *Science* **2013**, *341*, 984; b) G. Huang, Q. Yang, Q. Xu, S. H. Yu, H. L. Jiang, *Angew. Chem.* **2016**, *128*, 7505; *Angew. Chem., Int. Ed. Engl.* **2016**, *55*, 7379; c) W. Wang, Y. Zhang, W. Liu, *Prog. Polym. Sci.* **2017**, *71*, 1; d) P. Lin, T. Zhang, X. Wang, B. Yu, F. Zhou, *Small* **2016**, *12*, 4386.

[8] a) D. G. Barrett, G. G. Bushnell, P. B. Messersmith, *Adv. Healthcare Mater.* **2013**, *2*, 745; b) H. Kamata, Y. Akagi, Y. Kayasuga-Kariya, U.-i. Chung, T. Sakai, *Science* **2014**, *343*, 873; c) V. X. Truong, M. P. Ablett, S. M. Richardson, J. A. Hoyland, A. P. Dove, *J. Am. Chem. Soc.* **2015**, *137*, 1618.

[9] H. Kamata, K. Kushiro, M. Takai, U. i. Chung, T. Sakai, *Angew. Chem.* **2016**, *128*, 9428; *Angew. Chem., Int. Ed.* **2016**, *55*, 9282.

[10] Y. Bai, B. Chen, F. Xiang, J. Zhou, H. Wang, Z. Suo, *Appl. Phys. Lett.* **2014**, *105*, 151903.

[11] G. M. Peters, L. P. Skala, T. N. Plank, H. Oh, G. Manjunatha Reddy, A. Marsh, S. P. Brown, S. R. Raghavan, J. T. Davis, *J. Am. Chem. Soc.* **2015**, *137*, 5819.

[12] a) H. Yuk, S. Lin, C. Ma, M. Takaffoli, N. X. Fang, X. Zhao, *Nat. Mater.* **2017**, *8*; b) S. Y. Chin, Y. C. Poh, A.-C. Kohler, J. T. Compton, L. L. Hsu, K. M. Lau, S. Kim, B. W. Lee, F. Y. Lee, S. K. Sia, *Sci. Rob.* **2017**, *2*, eaah6451.

[13] a) M. Liu, L. Jiang, *Sci. China Mater.* **2016**, *59*, 239; b) M. Liu, S. Wang, L. Jiang, *Nat. Rev. Mater.* **2017**, *2*, 17036; c) J. Ryu, S. H. Ku, H. Lee, C. B. Park, *Adv. Funct. Mater.* **2010**, *20*, 2132; d) M. H. Ryou, J. Kim, I. Lee, S. Kim, Y. K. Jeong, S. Hong, J. H. Ryu, T. S. Kim, J. K. Park, H. Lee, *Adv. Mater.* **2013**, *25*, 1571.

[14] a) Z. Zhao, R. Fang, Q. Rong, M. Liu, *Adv. Mater.* **2017**, *29*; b) H. Gao, Z. Zhao, Y. Cai, J. Zhou, W. Hua, L. Chen, L. Wang, J. Zhang, D. Han, M. Liu, *Nat. Commun.* **2017**, *8*, 15911.

[15] L. Chen, Y.-a. Yin, Y.-x. Liu, L. Lin, M.-j. Liu, *Chin. J. Polym. Sci.* **2017**, *35*, 1181.

[16] a) M. Liu, S. Wang, Z. Wei, Y. Song, L. Jiang, *Adv. Mater.* **2009**, *21*, 665; b) L. Lin, M. Liu, L. Chen, P. Chen, J. Ma, D. Han, L. Jiang, *Adv. Mater.* **2010**, *22*, 4826.

[17] C.-C. Peng, J. Kim, A. Chauhan, *Biomaterials* **2010**, *31*, 4032.

[18] a) J. M. Berg, L. T. Eriksson, P. M. Claesson, K. G. N. Borve, *Langmuir* **1994**, *10*, 1225; b) E. A. Vogler, *Adv. Colloid Interface Sci.* **1998**, *74*, 69; c) R.-H. Yoon, D. H. Flinn, Y. I. Rabinovich, *J. Colloid Interface Sci.* **1997**, *185*, 363; d) A. J. Patel, P. Varilly, D. Chandler, *J. Phys. Chem. B* **2010**, *114*, 1632; e) C. Guo, S. Wang, H. Liu, L. Feng, Y. Song, L. Jiang, *J. Adhes. Sci. Technol.* **2008**, *22*, 395.

[19] P.-G. De Gennes, *Rev. Mod. Phys.* **1985**, *57*, 827.

[20] a) T. Du, S. Ma, X. Pei, S. Wang, F. Zhou, *Small* **2017**, *13*, 160202; b) J. Wang, L. Sun, M. Zou, W. Gao, C. Liu, L. Shang, Z. Gu, Y. Zhao, *Sci. Adv.* **2017**, *3*, e1700004.

[21] X. Yao, Y. Hu, A. Grinthal, T.-S. Wong, L. Mahadevan, J. Aizenberg, *Nat. Mater.* **2013**, *12*, 529.

Editorial Office:
Wiley-VCH Verlag
Boschstraße 12, 69469 Weinheim
Germany

Tel.: (+49) 6201 606 531
Fax: (+49) 6201 606 500

Email: afm@wiley-vch.de
http://www.afm-journal.com

Reprint Order Form 2018

Short DOI: adfm. _____

Please send me and bill me for

☐ **Reprints** via ☐ airmail (+ 25 Euro)
☐ surface mail

Please send me and bill me for a:

☐ **Issue copies** (25 Euro)

☐ **high-resolution PDF file** (330 Euro).

My Email address:

_____

Please note: It is not permitted to present the PDF file on the internet or on company homepages.

Information regarding VAT

Please note that from German sales tax point of view, the charge for **Reprints, Issues or Posters** is considered as **"supply of goods"** and therefore, in general, such delivery is a subject to German sales tax. However, this regulation has no impact on customers located outside of the European Union. Deliveries to customers outside the Community are automatically tax-exempt. Deliveries within the Community to institutional customers outside of Germany are exempted from the German tax (VAT) only if the customer provides the supplier with his/her VAT number. The VAT number (value added tax identification number) is a tax registration number used in the countries of the European Union to identify corporate entities doing business there. It starts with a country code (e.g. FR for France, GB for Great Britain) and follows by numbers.

VAT no.: _____

(Institutes / companies in EU countries only)

Purchase Order No.: _____

Delivery address / Invoice address:
Name of recipient, University, Institute, Street name and Street number, Postal Code, Country

_____

_____

_____

_____

_____

_____

_____

Date and Signature: _____

Credit Card Payment (optional) -You will receive an invoice.

VISA, MasterCard, AMERICAN EXPRESS

Please use the Credit Card Token Generator located at the website below to create a token for secure payment. The token will be used instead of your credit card number.

Credit Card Token Generator:
https://www.wiley-vch.de/editorial_production/index.php

Please transfer your token number to the space below.

Credit Card Token Number

Price list for reprints (The prices include mailing and handling charges. All Wiley-VCH prices are exclusive of VAT)

No. of pages	Price (in Euro) for orders of 50 copies	100 copies	150 copies	200 copies	300 copies	500 copies
1-4	345	395	425	445	548	752
5-8	490	573	608	636	784	1077
9-12	640	739	786	824	1016	1396
13-16	780	900	958	1004	1237	1701
17-20	930	1070	1138	1196	1489	2022
for every additional 4 pages	147	169	175	188	231	315

Wiley-VCH Verlag GmbH & Co. KGaA; Location of the Company: Weinheim, Germany;
Trade Register: Mannheim, HRB 432833, Chairman of the Board: Mark Allin
General Partner: John Wiley & Sons GmbH, Location: Weinheim, Germany
Trade Register Mannheim, HRB 432296,
Managing Directors: Sabine Steinbach, Dr. Guido F. Herrmann

WILEY-VCH